HDR Image Watermarking based on Bracketing Decomposition

Vassilios Solachidis, Emanuele Maiorana, Patrizio Campisi
Department of Engineering
University Roma Tre
Rome, Italy
vassilios.s@gmail.com, maiorana@uniroma3.it, campisi@uniroma3.it

Francesco Banterle
Visual Computing Lab
ISTI-CNR
Pisa, Italy
frabante@gmail.com

***Abstract*—The present paper proposes a novel watermarking scheme specifically designed for high dynamic range (HDR) images. The employed embedding strategy is based on a decomposition of the original HDR representation into multiple low dynamic range (LDR) images by means of a bracketing process. After having inserted the selected watermark into each LDR component, the final output is generated by combining the available contributions into a single HDR object. By exploiting some of the well studied properties of digital watermarking for standard LDR images, our approach is able to generate a watermarked HDR image visually equivalent to the original one, while allowing to detect the embedded information in both the marked HDR image and in its LDR counterpart, obtained through tone-mapping operators or by extracting a specific luminance range of interest from it. Several results obtained from an extensive set of experimental tests are reported to testify the effectiveness of the proposed scheme.**

***Index Terms*—High dynamic range (HDR) imaging; tone-mapping operators (TMOs); watermarking; data hiding.**

I. Introduction

High dynamic range (HDR) imaging consists of a set of digital processing and photographic methods used for generating and reproducing real scene representations characterized by a dynamic range far greater than the one provided by current standard imaging approaches [1], commonly indicated as low dynamic range (LDR) methods. Through HDR based techniques, it is in fact possible to accurately represent real scenarios with their entire range of intensity levels, by typically combining into a single object the information acquired from both very dark areas of the observed scene, using high exposures settings, and also very bright areas by exploiting low camera exposure values [2]. It is worth pointing out that HDR images cannot be reproduced by means of conventional displays since they are unable to render highly contrasted images with maximum luminance usually greater than 1000 cd/m^2. Dedicated HDR displays, commonly based on the modulation of the reproduced intensity through a back-light illumination, are therefore under development for guaranteeing a proper viewing experience of HDR images [3]. Nevertheless, such devices are available only for either professional or experimental use due to their high cost [4]. Therefore, the modality with which HDR images can be nowadays usually experienced requires the use of tone-mapping operators (TMOs), whose aim is to reduce the strong global contrast of the original scene while trying to locally preserve the most relevant image details and color appearance, thus allowing to display the resulting LDR image on standard viewing displays [5].

The present paper deals with the issue of providing the means for properly protecting the intellectual property of HDR images, by proposing a novel watermarking scheme specifically designed for this kind of images. It is in fact worth pointing out that, with respect to LDR images which often suffer from loss of details in either the brightest or darkest areas of a scene, HDR images are much more valuable in terms of quantity and quality of the carried information, which makes them an extremely interesting target for misappropriation or misuse by malevolent entities. Digital watermarking is a possible countermeasure against such threats: it consists in the insertion of a watermark into an HDR image, which has to be realized without significantly altering the image visual appearance, while allowing its detection after any processing which do not significantly alter the quality of the original data. In general, watermarking approaches have been extensively applied in the last decade to LDR images [6], [7], and employed for a wide range of applications ranging from the protection of the intellectual property of 2D [8] or 3D images [9], [10], to unconventional image compression [11], copyright protection of vector graphics [12], or even biometric applications [13], just to cite a few. However, when defining a watermarking scheme for HDR images, specific issues have to be taken into account: first of all, the characteristics of the human visual system (HVS) which have to be taken into account for imperceptibly embedding a message, may vary greatly for distinct HDR images, due to the fact that their luminance values may be in significantly different ranges, while LDR images are commonly represented in a fixed range, i.e. [0,255]. Moreover, it has to be guaranteed that the embedded information may be detectable from any image obtained through either malicious or non-malicious modifications of the HDR content retaining the most of the originally available visual information. This means that a desired requirement for an HDR watermarking scheme is the robustness against non-linear distortion such as those performed by TMOs, and possibly also against any process generating LDR images by taking into account a specific range of luminance values of interest. These requirements are actually taken into account

978-1-4673-5807-1/13/$31.00 ©2013 IEEE DSP2013

in the design of the watermarking framework here proposed, which is based on the decomposition of the original HDR data into multiple LDR samples, and on the embedding of the watermark in each of the so-generated contributions.

The present paper is organized as follows: a review on the state-of-the-art on HDR image data hiding is provided in Section II. The proposed approach is then detailed in Section III, while the experimental tests conducted to verify its effectiveness are described in Section IV. Eventually, some conclusions are reported in Section V.

II. Data Hiding for HDR images

Despite HDR imaging is rapidly emerging as an innovative approach for representing real scenes characterized by significant contrast, there is still a very limited number of papers dealing with data hiding in HDR images. Specifically, a steganographic approach is presented in [14], where a message is embedded inside an HDR image by selecting the exponent of each pixel according to the bits which have to be transmitted, and changing the corresponding mantissa in order to maintain the same original color, thus exploiting the peculiar characteristic of the RGBe encoding format of specifying a given color with different possible representations. Marked images are therefore obtained in a distortion-free modality, although an analysis on the statistics of the modified exponents of the employed format is not carried out. Another steganographic method is presented in [15], where each image pixel is classified either in a flat or in a boundary area, before determining the capacity of the message embedded in each pixel according to its contrast and luminance.

A single bit HDR watermarking method is presented in [16], where the approximation subband of the LogLUV domain wavelet decomposition is selected as embedding domain, and the kurtosis of different areas is modified in order to assume a specific value determined by a quantization-index-modulation (QIM) non-uniform quantizer. The method imperceptibility is evaluated through the HDR-VDP metrics [17]. A watermarking framework where a TMO is applied to the original HDR image to compute its LDR version and the watermark is embedded in it using any conventional LDR image watermarking method, is given in [18]. The final watermarked HDR image is then generated as the product of the watermarked LDR image and the ratio between the original and unmarked HDR and LDR images. Since the range of HDR images is orders of magnitude greater than the one of LDR images, the ratio between them will be high in correspondence of areas with high luminance, where the watermark will be therefore very intense. Similarly, other two methods are presented in [19]: the first one based on the μ-Law, employed as a generic TMO to produce an LDR image, and the second one on bilateral filtering. Both approaches generates an LDR image which is multiplicatively watermarked before multiplying it with the residual from the HDR domain. Eventually, a blind multi-bit watermarking exploiting the just noticeable difference (JND) scaled space as embedding domain and a visual mask based on bilateral filtering and on a contrast sensitivity function is proposed in [20].

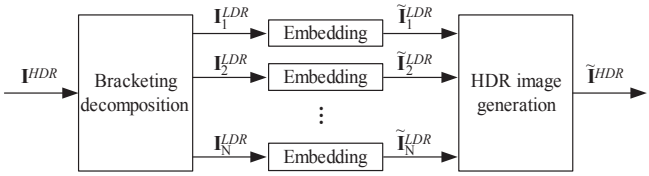

Fig. 1: Proposed watermark embedding procedure.

It is worth observing that the robustness of the embedded watermarks is evaluated in [16], [18]–[20] only with respect to the application of TMOs, while the possibility of detecting the watermark from an LDR image obtained with specific reference to only a specific range of luminance has not been considered so far. This case is considered for testing the performance of the proposed approach in Section IV.

III. Proposed Approach for HDR image watermarking

The proposed framework for HDR image watermarking is detailed in this Section. Specifically, the employed embedding procedure is described in Section III-A, while the detection phase is illustrated in Section III-B.

A. Watermark embedding

The proposed watermark embedding procedure is sketched in Figure 1. It consists of three steps: 1) performing the decomposition of the HDR image into several LDR components, 2) watermark embedding in each generated LDR image, 3) HDR image reconstruction. The entire watermarking process is performed on the luminance component of the considered HDR image, while the chrominance components are left untouched. Such choice is driven by the fact that the most of the perceptual information of an image is in its luminance component, for which therefore more accurate perceptibility models are available. Moreover, TMOs are commonly applied to the luminance component in order to retain the most of the associated information, while their behavior on the chromaticity components is often unpredictable. The details on each step are given in the following sections.

1) HDR image bracketing decomposition: The original HDR image is first decomposed into a number of different LDR contributions according to the bracketing procedure described in this section. This procedure aims at reproducing the process through which HDR images of real scenarios are created, that is, by generating multiple LDR samples from a single scene, each containing a specific range of the available luminance dynamics. The same operation is performed in our approach having as target the HDR image rather than the real scene. Specifically, given an HDR image with its associated dynamic range, the number N of LDR samples into which the original data is decomposed depends on the ratio between the maximum and minimum luminance characterizing a single LDR contribution, and on the ratio between the minimum luminance associated with two consecutive LDR

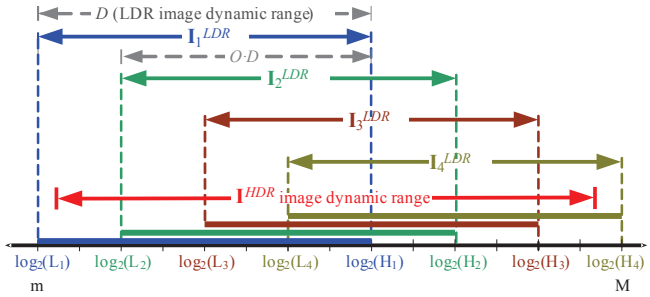

Fig. 2: Dynamic range bracketing decomposition: several LDR images are generated by selecting different luminance ranges.

Fig. 3: Example of a bracketing decomposition: each tile is taken from one of the six LDR images generated from the same HDR data.

images. Adopting a representation similar to the one commonly employed in photography, these ratios can be expressed in terms of powers of two, respectively as 2^D and $2^{D(1-O)}$, $0 < O < 1$. This way, the parameters D and O are employed in our approach for representing the dynamic range of each LDR image and the overlap percentage between consecutive LDR images respectively, as visually described in Figure 2. The exponent D can be measured in terms of *f-stop*, the unit commonly employed to quantify ratios in photography.

Having indicated as $\mathbf{I}^{HDR}$ the luminance of the original HDR image, its dynamic range can be expressed through its minimum and maximum values, which are given in terms of logarithms to base two as $m = \lfloor \log_2(\min\{\mathbf{I}^{HDR}\}) \rfloor$ and $M = \lceil \log_2(\max\{\mathbf{I}^{HDR}\}) \rceil$, respectively. The $i-th$ LDR image $\mathbf{I}_i^{LDR}$, with $i = 1, \ldots, N = \lceil \frac{M-m}{D(1-O)} \rceil$, is then generated in order to assume, for each pixel $\mathbf{x}$, the value

$$\mathbf{I}_i^{LDR}(\mathbf{x}) = \begin{cases} 0 & , \ \mathbf{I}^{HDR}(\mathbf{x}) \leq L_i \\ 255 \cdot \left[\frac{\mathbf{I}^{HDR} - L_i}{H_i - L_i} \right]^{\gamma} & , \ L_i < \mathbf{I}^{HDR}(\mathbf{x}) \leq H_i \\ 255 & , \ H_i < \mathbf{I}^{HDR}(\mathbf{x}) \end{cases} \quad (1)$$

where $\gamma < 1$ is the exponent employed for adapting the luminance values to the properties of human vision by means of a *gamma correction* function, while $L_i = 2^{m+D\cdot(i-1)\cdot(1-O)}$ and $H_i = 2^{m+D\cdot[(i-1)\cdot(1-O)+1]}$ are respectively the lowest and highest original luminance values reported in the $i-th$ LDR image $\mathbf{I}_i^{LDR}$, with $H_i/L_i = 2^D$ and $L_{i+1}/L_i = 2^{D(1-O)}$ as already mentioned.

In case $O = 0$ there is no overlap between two distinct LDR images ($H_i/L_i = L_{i+1}/L_i = 2^D$), and then each pixel of the original HDR image contributes to only one LDR component, being clamped in all the other LDR images. Furthermore, in this case the number $N = \lceil \frac{M-m}{D} \rceil$ of generated LDR images takes its lowest possible value. On the other hand, the number of LDR images increases together with O, till reaching very high values when $O \to 1$. An example of the bracketing decomposition of an HDR image is illustrated in Figure 3, which shows a tiling of six LDR images obtained with parameters $D = 4$ and $O = 0.4$.

2) Embedding strategy: Once several LDR images are generated from the original HDR one, LDR watermarking approaches can be employed, thus relying on the available knowledge on perceptual models for LDR images in order to guarantee the imperceptibility of the embedded mark. This way, it could be easier to ensure the perceptual quality not only of the final watermarked HDR image, but also of any LDR object derived from it by applying tone-mapping or bracketing operations.

The watermarking strategy proposed in [21] is used in this paper. Specifically, the considered watermark $\mathbf{w}$ is assumed to be a random bi-valued signal with values equal to ± 1, and it is additively embedded in the first-level decomposition subbands obtained by applying a discrete wavelet transform (DWT) on each LDR image $\mathbf{I}_i^{LDR}$, $i = 1, \ldots, N$. In more details, the embedding is performed as:

$$\tilde{\mathbf{I}}_{i,\theta}^{LDR}(\mathbf{x}) = \mathbf{I}_{i,\theta}^{LDR}(\mathbf{x}) + \lambda \cdot \mathbf{f}_\theta(\mathbf{x}) \cdot \mathbf{w}_\theta(\mathbf{x}), \quad (2)$$

where $\mathbf{I}_{i,\theta}^{LDR}$ is the first-level wavelet decomposition subband with orientation $\theta \in \Theta = \{LH, HL, HH\}$ of the LDR image $\mathbf{I}_i^{LDR}$, and $\tilde{\mathbf{I}}_{i,\theta}^{LDR}$ its watermarked counterpart. The watermark strength is determined by λ, while $\mathbf{w}_\theta$ is the portion of the mark embedded in the θ-subband, with $\mathbf{w} = [\mathbf{w}_{LH} \ \mathbf{w}_{HL} \ \mathbf{w}_{HH}]$. As for the term $\mathbf{f}_\theta$, it is employed as a weighting function depending on the human sensitivity to some image characteristics, and it is expressed as

$$\mathbf{f}_\theta(\mathbf{x}) = \frac{1}{2} \cdot \Psi(\theta) \cdot \Upsilon(\mathbf{x}) \cdot \Xi(\mathbf{x})^{0.2} \quad (3)$$

where $\Psi(\theta)$ is related to the sensitivity to noise changes in the θ-subband, $\Upsilon(\mathbf{x})$ expresses the local sensitivity on brightness, while $\Xi(\mathbf{x})$ depends on the local texture activity. Further details on the above expressions can be found in [21]. The marked images $\tilde{\mathbf{I}}_i^{LDR}$, $i = 1, \ldots, N$, are then obtained by applying an inverse DWT to their available wavelet decompositions, and clamped to the allowed range [0,255] in case any value exceeds such limits. Moreover, in order to reconstruct a proper watermarked HDR image, we also need to force $\tilde{\mathbf{I}}_i^{LDR}(\mathbf{x}) = \mathbf{I}_i^{LDR}(\mathbf{x})$ for all the pixels $\mathbf{x}$ such that $\mathbf{I}_i^{LDR}(\mathbf{x})$ is equal to either 0 or 255. It has also to be specified that the watermark is embedded only in the LDR images having a percentage of non-clamped pixels, having value different from either 0 or 255, greater than 10%, as made evident from the detection phase described in Section III-A3.

3) Watermarked HDR image generation: Once the watermark is embedded in each of the N LDR images $\tilde{\mathbf{I}}_i^{LDR}$, $i = 1, \ldots, N$, the final output can be generated by blending the available contributions into a single HDR image $\tilde{\mathbf{I}}^{HDR}$. Actually, each LDR contribution $\tilde{\mathbf{I}}_i^{LDR}$ can be exploited only within its associated range $[L_i, H_i]$ described in Section III-A1. Indeed, as can be seen from (1), values in $\tilde{\mathbf{I}}_i^{LDR}$ equal to either 0 or 255 refer to cases in which the luminance of the original HDR image has been clamped, and should be therefore discarded during the reconstruction process. The final watermarked HDR image $\tilde{\mathbf{I}}^{HDR}$ has to be then computed as

$$\tilde{\mathbf{I}}^{HDR}(\mathbf{x}) = \frac{1}{|C_{\mathbf{x}}|} \sum_{i \in C_{\mathbf{x}}} L_i + (H_i - L_i) \cdot \left[\frac{\tilde{\mathbf{I}}_i^{LDR}(\mathbf{x})}{255}\right]^{\frac{1}{\gamma}} \quad (4)$$

where $C_{\mathbf{x}} = \{i : 0 < \tilde{\mathbf{I}}_i^{LDR}(\mathbf{x}) < 255\}$ is the set containing the indexes corresponding to the LDR images $\tilde{\mathbf{I}}_i^{LDR}(\mathbf{x})$ for which the pixel $\mathbf{x}$ has not been clamped, and $|C_{\mathbf{x}}|$ its cardinality. The most of the watermark is therefore embedded in the dynamic ranges resulting in the lowest number of clamped pixels, which usually correspond to the central considered ranges, as can be also seen from the example reported in Figure 3.

B. Watermark Detection

According to the employed watermark embedding strategy, also the proposed detection method is derived from the one presented in [21]: the correlation between the considered image and the watermark is evaluated. More specifically, when adopting the approach described in Section III-A for marking HDR images, the detection phase can be performed either directly on the marked HDR image, or on each LDR image obtained by applying the bracketing decomposition process described in Section III-A1 to the marked HDR image. In more details, three different strategies are evaluated for detecting the presence of a watermark $\hat{\mathbf{w}}$ inside a watermarked image $\tilde{\mathbf{I}}^{HDR}$:

1) Detector 1 (LogHDR): the detection is directly performed on the HDR image, by first taking its logarithm $\mathbf{L} = log(\tilde{\mathbf{I}}^{HDR})$ and then computing its DWT first level decomposition $\mathbf{L}_\theta$, $\theta \in \Theta$. The logarithm transform is adopted as in [22], where it is exploited to describe the effects of a generic TMO. As in [21], the detector output is obtained by first evaluating the correlation as the average $\mathcal{E}_{\mathbf{x},\theta}\{\mathbf{L}_\theta(\mathbf{x}) \cdot \hat{\mathbf{w}}_\theta(\mathbf{x})\}$ of the product $\mathbf{L}_\theta(\mathbf{x}) \cdot \hat{\mathbf{w}}_\theta(\mathbf{x})$ over all the admissible values of $\mathbf{x}$ and θ, and by the performing score normalization by dividing the evaluated correlation with the standard deviation $\sqrt{\mathcal{E}_{\mathbf{x},\theta}\{[\mathbf{L}_\theta(\mathbf{x})]^2\}}$;
2) Detector 2 (MeanLDR): the detection is performed by first applying to $\tilde{\mathbf{I}}^{HDR}$ a bracketing process with the same parameters D and O employed during embedding, thus obtaining N LDR images $\tilde{\mathbf{I}}_i^{LDR}$. The DWT decomposition of each LDR image is then computed, and N different scores are evaluated as $s_i = \mathcal{E}_{\mathbf{x},\theta}\{\tilde{\mathbf{I}}_{i,\theta}^{LDR}(\mathbf{x}) \cdot \hat{\mathbf{w}}_\theta(\mathbf{x})\} / \mathcal{E}_{\mathbf{x},\theta}\{[\tilde{\mathbf{I}}_{i,\theta}^{LDR}(\mathbf{x})]^2\}$, $i = 1, \ldots, N$. Eventually, the mean of the N evaluated scores is taken as the final output of the detector. It is worth specifying that the LDR images considered for evaluating the final score are only those having a percentage of non-clamped pixels greater than 10%;
3) Detector 3 (MaxLDR): as for the second detector, N LDR images are first generated by applying the bracketing process described in Section III-A1. Then, the final output is obtained in this case as the maximum score $\max_{i \in \{1,\ldots,N\}}\{s_i\}$ among all the evaluated normalized correlations.

ID	Image name	Dynamic range	Size	N		
				D=6	D=8	D=10
1	AtriumMorning	$1.98{\cdot}2^{14}$	1016×760	6	5	4
2	AtriumNight	$1.6 \cdot 2^{28}$	1016×760	9	7	6
3	mpi_atrium_1	$1.47{\cdot}2^{14}$	676×1024	5	4	3
4	nancy_cathedral_1	$1.59{\cdot}2^{14}$	2048×1536	5	4	3
5	nancy_cathedral_2	$1.93{\cdot}2^{14}$	2048×1536	7	5	4
6	snow	$1.02{\cdot}2^{10}$	1536×2048	4	3	3

TABLE I: Employed HDR images with corresponding details. The last three columns report the number of LDR images generated for different D values, while keeping O=0.3.

For all the considered strategies, the watermark is assumed to be detected if the computed output is greater than a given detection threshold. In case the watermark is detected from an LDR image, obtained from the marked corresponding HDR by applying a TMO or by just extracting the information from a selected luminance range, the same output produced by the second and third detectors is directly evaluated, with the only difference that a single score can be now derived from the only available LDR image.

IV. Experimental Tests

An extensive set of experimental tests is carried out to evaluate the performance of the proposed bracketing-based watermarking approach for HDR images. Specifically, the six images listed in Table I are taken from [23] and used as dataset. The employed images contain real luminance values expressed in cd/m^2, being thus possible to apply the proposed method to them, and to exploit the HDR-VDP-2 metric [24] to evaluate the perceptibility of the embedded watermarks. In more detail, the HDR-VDP-2 objective metric is used to control the watermarking strength λ in (2), which is adjusted in order to produce marked HDR images for which the probability of detecting a difference from the original image is less than 5% for the 90% of the image pixels. Such requisite actually correspond to a perceptual quality for which it is normally not possible to detect any difference between the original and the marked HDR image according to the HDR-VDP metrics [17], which has been considered for evaluating the watermark imperceptibility in [16].

The performance dependence on the bracketing parameters D and O, and on the employed detection strategy, is first analyzed. To this aim, each considered image is watermarked with a random key $\mathbf{w}$, and the detection is then performed with the same key employed during embedding ($\hat{\mathbf{w}} = \mathbf{w}$) and also with a different one ($\hat{\mathbf{w}} \neq \mathbf{w}$). This process is repeated

Dynamic range D	Overlap percentages O			
	0.1	0.2	0.3	0.4
	Detector 1 (LogHDR)			
6	-21.7	-29.4	-32.3	-31
8	-11.2	-16.3	-21.9	-25.7
10	-9.3	-28.4	-28.9	-32.1
	Detector 2 (MeanLDR)			
6	-9.2	-18.5	-26.1	-27.4
8	-6.8	-15.9	-14.7	-18.8
10	-4.2	-9.2	-8.9	-8.4
	Detector 3 (MaxLDR)			
6	-12.3	-20.8	-33.3	-37.1
8	-7	-19.4	-19.5	-20.5
10	-4.1	-7.9	-7.6	-14.4

TABLE II: Performance (in terms of $log_{10}(P_{miss})$) dependence on the system parameters and the employed detector strategy for HDR images.

for 100 different keys in order to generate, for each detector described in Section III-B, two distributions corresponding to the scores available when performing detection with the same key employed during embedding or with a different one.

Assuming that these distributions are Gaussian, we can evaluate the probability of missed detection P_{miss} achievable in each configuration while having fixed the probability of false mark detection $P_{fa} = 10^{-5}$ and the corresponding detection threshold. The obtained values are reported in Table II, from which it can be seen that the best performance is achieved when using the MaxLDR detector and $D = 6$ and $O = 0.4$ as bracketing parameters, which therefore represents the system configuration considered in the following. From the performed test, it is possible to check that, in general, the detection performance improves when increasing the overlap parameter O and decreasing the range parameter D. However, further increasing O or decreasing D results in a significant growth of the number of generated LDR images, and of the requested computational complexity with it, without further significant performance improvements. For the sake of comparison, in case no bracketing is applied during the embedding phase, thus the mark simply inserted into the gamma-corrected HDR image, the best achievable performance for $P_{fa} = 10^{-5}$ correspond to $P_{miss} = 1.6 \cdot 10^{-6}$, thus resulting in a far worse behavior than the one provided by the proposed bracketing decomposition strategy.

In order to assess the robustness of the proposed approach, the performance achievable when detecting the embedded mark from LDR images is also evaluated. Specifically, the possibility of performing detection on the tone-mapped versions of the watermarked HDR images is first analyzed in Table III which reports, for each considered image, the detection performance in terms of equal error rate (EER), which corresponds to the condition in which $P_{miss} = P_{fa}$. The EER achieved on the individual HDR images is also reported for reference.

TMO	Images (ID)					
	1	2	3	4	5	6
HDR (no TMO)	-17.8	-25.2	-17.5	-203.7	-71.7	-31.3
tonemap [25]	-20.3	-28.4	-22.8	-156.0	-79.5	-27.0
iCAM06 [26]	-15.5	-35.8	-15.1	-95.7	-70.7	-40.6
Drago [5]	-20.5	-22.0	-19.0	-153.7	-88.6	-12.7
Reinhard [5]	-13.2	-25.8	-14.3	-167.9	-75.3	-17.7
TR [5]	-8.4	-23.3	-11.5	-160.9	-66.7	-11.0

TABLE III: Performance (in terms of $log_{10}(EER)$) for mark detection from both HDR images and LDR images obtained through different TMOs.

Eventually, we also consider the case in which an LDR image is derived from the marked HDR data by considering only a specific range of luminance values. Such processing can be performed when the information of interest resides only within a given luminance dynamic whose contrast has to be maximized in the LDR representation, with the requirement of maintaining the watermark in it. In order to investigate this scenario, the performance achievable when decomposing the marked HDR image into LDR representations with a dynamic range D' different from the one employed during the embedding is evaluated. Specifically, Figure 4 shows the EERs estimated for different LDR representations extracted from a marked HDR image, when considering either a larger ($D' = D + \sqrt{2} = 7.41$) or a narrower ($D' = D - \sqrt{2} = 4.28$) dynamic range than the one used for embedding, which is $D = 6$ (the overlap percentage is kept as $O = 0.4$). The results for only three out of the six analyzed images are reported because of space constraint, however the observed behavior is common for all the considered images. The number of LDR images produced in each scenario depends on the entire dynamic range of the considered images, as well as on the employed parameter D'. Together with the EER, also the percentage of clamped pixels in each LDR image is reported in Figure 4, thus showing a strict dependance between this percentage and the detection performance, which are usually worse when considering images with a large number of clamped pixels. From the reported results it is possible to verify that very good performance can be achieved also when dealing with LDR images obtained by isolating a dynamic range different from those considered during embedding, while guaranteeing an EER lower than 10^{-2} for all the LDR images with a percentage of non-clamped pixels greater than 10%.

V. Conclusions

A watermarking framework for HDR images based on bracketing decomposition has been presented in this paper. According to the proposed approach, a watermark is embedded in all the LDR images obtained by dividing the original HDR information into different luminance ranges, thus allowing to exploit the well-studied perceptual properties of LDR images for watermark embedding. Several experimental tests have confirmed that the proposed method can ensure very good detection rates while guaranteeing the imperceptibility of the embedded mark, being also robust against both tone-mapping and bracketing procedures, which generate LDR versions of

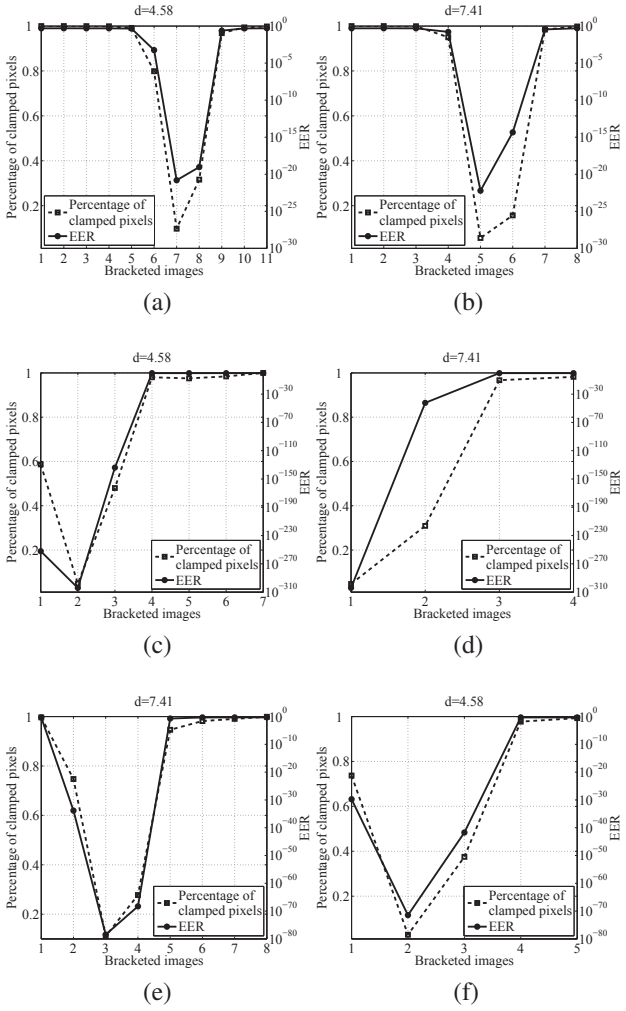

Fig. 4: Percentage of clamped pixels and detection performance (in terms of EER) for LDR images generated by extracting a specific range of luminance (with either $D = 4.58$ or $D = 7.41$) from the watermarked HDR image. (a),(b): Image 2; (c),(d): Image 4; (e),(f): Image 5.

the original data from which it is still possible to retrieve the embedded messages.

ACKNOWLEDGMENT

This work has been partially supported by the EU FP7 Marie Curie IAPP project DIVeFor "Digital Image and Video Forensics" (Grant Agreement No. 251677). The authors also acknowledge the EU COST Action IC1005 "HDRi: The digital capture, storage, transmission and display of real-world lighting".

REFERENCES

[1] E. Reinhard, W. Heidrich, S. Pattanaik, P. Debevec, G. Ward, and K. Myszkowski, *High Dynamic Range Imaging: Acquisition, Display, and Image-Based Lighting*, Morgan Kaufmann series in computer graphics. Elsevier Science, 2010.

[2] P.E. Debevec and J. Malik, "Recovering high dynamic range radiance maps from photographs," in *Proc. of ACM SIGGRAPH*, 1997.

[3] H. Seetzen, W. Heidrich, W. Stuerzlinger, G. Ward, L. Whitehead, M. Trentacoste, A. Ghosh, and A. Vorozcovs, "High dynamic range display systems," *ACM Trans. on Graphics*, vol. 23, no. 3, pp. 760–768, 2004.

[4] "SIM2 HDR display series," http://www.sim2.com/HDR/, retrieved April, 2013.

[5] F. Banterle, A. Artusi, K. Debattista, and A. Chalmers, *Advanced High Dynamic Range Imaging: Theory and Practice*, AK Peters (CRC Press), Natick, MA, USA, 2011.

[6] F. Barni and F. Bartolini, *Watermarking Systems Engineering: Enabling Digital Assets Security and Other Applications*, CRC Press, 2004.

[7] I. J. Cox, M. Miller, J.A. Bloom, J. Fridrich, and T. Kalker, *Digital Watermarking and Steganography*, Morgan Kaufmann, 2008.

[8] Y. Zhao, P. Campisi, and D. Kundur, "Dual domain watermarking for authentication and compression of cultural heritage images," *IEEE Trans. on Image Processing, Special Issue on Cultural Heritage*, vol. 13, no. 3, pp. 430–448, 2004.

[9] P. Campisi, "Object oriented stereo image digital watermarking," *SPIE Journal of Electronic Imaging*, vol. 17, no. 4, 2008.

[10] V. Solachidis and I. Pitas, "Watermarking digital 3-D volumes in the discrete fourier transform domain," *Multimedia, IEEE Trans. on*, vol. 9, no. 7, pp. 1373–1383, 2007.

[11] P. Campisi, D. Kundur, D. Hatzinakos, and A. Neri, "Compressive data hiding: An unconventional approach for improved color image coding," *EURASIP Journal on Applied Signal Processing, Special issue on Emerging Applications of Multimedia Data Hiding*, vol. 2002, no. 2, pp. 152–163, 2002.

[12] V. Solachidis and I. Pitas, "Watermarking polygonal lines using Fourier descriptors," *IEEE Computer Graphics and Applications*, vol. 24, no. 3, pp. 44–51, 2004.

[13] E. Maiorana, P. Campisi, and A. Neri, "Biometric signature authentication using Radon transform-based watermarking techniques," in *IEEE Biometrics Symposium*, September 2007.

[14] Chung-Min Yu, Kuo-Chen Wu, and Chung-Ming Wang, "A distortion-free data hiding scheme for high dynamic range images," *Displays*, vol. 32, no. 5, pp. 225 – 236, 2011.

[15] Yu-Ming Cheng and Chung-Ming Wang, "A novel approach to steganography in high- dynamic-range images," *Multimedia, IEEE*, vol. 16, no. 3, pp. 70 –80, july-sept. 2009.

[16] F. Guerrini, M. Okuda, N. Adami, and R. Leonardi, "High dynamic range image watermarking robust against tone-mapping operators," *IEEE Trans. on Information Forensics and Security*, vol. 6, no. 2, pp. 283–295, June 2011.

[17] R. Mantiuk, S. Daly, K. Myszkowski, and H.-S. Seidel, "Predicting visible differences in high dynamic range images - model and its calibration," in *IS&T/SPIE's 17th Annual Symposium on Electronic Imaging 5666*, 2005.

[18] J.-L. Wu, "Robust watermarking framework for high dynamic range images against tone-mapping attacks," in *Watermarking - Volume 2*, pp. 229–242. InTech, 2012.

[19] X. Xue, T. Jinno, J. Xin, and M. Okuda, "Watermarking for HDR image robust to tone mapping," *IEICE Trans. on Fundamentals of Electronics, Communications and Computer Sciences*, vol. 94, no. 11, pp. 2334–2341, 2011.

[20] V. Solachidis, E. Maiorana, and P. Campisi, "HDR image multi-bit watermarking using bilateral-filtering-based masking," in *Proc. SPIE 8655, Image Processing: Algorithms and Systems XI, 865505*, February 2013.

[21] M. Barni, F. Bartolini, and A. Piva, "Improved wavelet-based watermarking through pixel-wise masking," *Image Processing, IEEE Trans. on*, vol. 10, no. 5, pp. 783–791, 2001.

[22] G.W. Larson, "LogLuv encoding for full-gamut, high-dynamic range images," *Journal of Graphics Tools*, vol. 3, no. 1, pp. 15–31, 1998.

[23] "http://www.mpi-inf.mpg.de/resources/hdr/gallery.html," .

[24] R. Mantiuk, K.J. Kim, A.G. Rempel, and W. Heidrich, "HDR-VDP-2: A calibrated visual metric for visibility and quality predictions in all luminance conditions," *ACM Trans. on Graphics*, vol. 30, no. 4, pp. 1–14, 2011.

[25] MATLAB, *version 7.10.0 (R2010a)*, The MathWorks Inc., Natick, Massachusetts, 2010.

[26] J. Kuang, G.M. Johnson, and M.D. Fairchild, "iCAM06: A refined image appearance model for HDR image rendering," *Journal of Visual Communication and Image Representation*, vol. 18, no. 5, pp. 406–414, 2007.